

Elementary Scaling Relations for Hall Effect Thrusters

Käthe Dannenmayer* and Stéphane Mazouffre†

Centre National de la Recherche Scientifique, 45071 Orléans, France

DOI: 10.2514/1.48382

Various sizing methodologies are currently available to get a first estimate of the required Hall effect thruster dimensions for a given input power and a corresponding thrust and specific impulse level. In this work, a semi-empirical approach to compute the three characteristic thruster dimensions, i.e., the channel length, the channel width, and the channel mean diameter, is introduced. The magnetic field strength is also considered. The determination of the scaling relations is based on analytical relationships deduced from the physical mechanisms that govern the properties of a Hall thruster discharge. A set of simplifying assumptions naturally specifies the validity domain of the relationships. The existence of a critical propellant atom density inside the channel, which warrants a high-efficiency thruster operation, is revealed and commented. The proportionality coefficients of the scaling relations are assessed by way of a vast database that comprises 33 single-stage Hall effect thrusters covering a power range from 10 W up to 50 kW. The sizing method is employed to access the geometry and the operating parameters for a 20 kW-class Hall thruster operating with xenon. Results obtained with two different series of simplifying assumptions are compared. The first set forms a very restrictive frame. The second set offers a more realistic description of the physics at work as the electron temperature, the energy losses and multiply charged ion species are taken into account.

Nomenclature

A	= channel cross section; area, m^2	n_n	= atom number density, m^{-3}
\mathbf{B}	= magnetic field, G	$n_{n,c}$	= critical atom density, m^{-3}
C_I	= proportionality coefficient for the discharge current	P, P_{in}	= discharge electrical power, overall input power, W
$C_{I_{sp}}$	= proportionality coefficient for the specific impulse	r, R	= inner, respectively, outer, channel radius, m
C_L	= proportionality coefficient for the channel length	r_{Le}	= electron Larmor radius, m
C_P	= proportionality coefficient for the power	S	= surface, m^2
C_{T1}, C_{T2}	= proportionality coefficient for the thrust	T	= thrust, N
C^*	= proportionality coefficient under low assumptions	T_e, T_n	= electron temperature, atom temperature, K
d, d_{ext}, d_{int}	= mean, external and internal channel diameter [m]	U_d	= discharge voltage, V
e	= elementary charge, C	v_e, v_n	= thermal speed of electrons and atoms, m/s
\mathbf{E}	= electric field, V/m	\bar{v}_i	= mean ion flow velocity, m/s
f_{2+}	= fraction of doubly charged ions	V	= volume, m^3
g_0	= Earth standard gravity, m/s^2	Z	= atomic number
h	= channel width, m	α	= propellant conversion efficiency
$I, I_d, I_e,$ I_{Hall}, I_i	= current, discharge current, electron current, Hall current, ion current, A	Δ	= voltage losses, V
I_{sp}	= specific impulse, s	η_A, η_T	= anode efficiency, thrust efficiency
j_{Hall}	= Hall current density, A/m^2	γ, γ'	= correction factors for the presence of multiply charged ions
k	= index number	λ_i	= ionization mean free path, m
k_B	= Boltzmann constant, J/K	ν_{en}	= electron–atom collision frequency, Hz
L	= channel length, m	ν_i	= ionization frequency, Hz
L_a	= acceleration layer length, m	π	= mathematical constant π
L_b	= magnetic layer characteristic size, m	ξ	= scaling index variable
$m_e, m_i, m_n,$ kg/s	= electron mass, ion mass, propellant atom mass, kg/s	σ_i	= cross section for ionization, m^2
\dot{m}_n, \dot{m}_i	= propellant mass flow rate through the anode, ion mass flow rate, kg/s	σ_{en}	= electron–atom momentum exchange cross section, m^2
		τ_{ce}	= gyroperiod, s
		τ_{en}	= electron–atom collisional time, s
		θ_d	= beam divergence correction term
		ω_{ce}	= electron cyclotron frequency, Hz

Received 3 December 2009; revision received 13 August 2010; accepted for publication 23 August 2010. Copyright © 2010 by S. Mazouffre. Published by the American Institute of Aeronautics and Astronautics, Inc., with permission. Copies of this paper may be made for personal or internal use, on condition that the copier pay the \$10.00 per-copy fee to the Copyright Clearance Center, Inc., 222 Rosewood Drive, Danvers, MA 01923; include the code 0748-4658/11 and \$10.00 in correspondence with the CCC.

*Ph.D. Student, Electric Propulsion Team, Institut de Combustion, Aérothermique, Réactivité et Environnement, 1C Avenue de la Recherche Scientifique; kathe.dannenmayer@cnrs-orleans.fr.

†Research Scientist, Electric Propulsion Team, Institut de Combustion, Aérothermique, Réactivité et Environnement, 1C avenue de la Recherche Scientifique; stephane.mazouffre@cnrs-orleans.fr.

I. Introduction

A HALL effect thruster (HET) is an advanced propulsion device that uses an electric discharge with magnetized electrons to ionize and accelerate a propellant gas [1,2]. Because of interesting features in terms of exit velocity, efficiency, thrust-to-power ratio and lifetime, HETs are recognized as an attractive propulsion means for missions and maneuvers that require a large velocity increment. A schematic of a Hall thruster is depicted in Fig. 1. The principle relies upon a magnetic barrier and a low-pressure DC discharge generated between an external cathode and an anode in such a way that a crossed electric and magnetic field discharge is created [1–4]. The anode, which also serves as gas injector, is located at the upstream

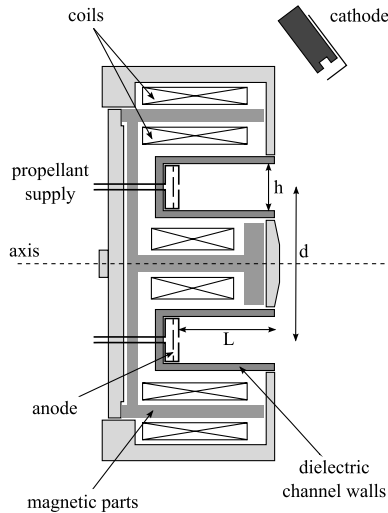


Fig. 1 Cross-section view of a Hall effect thruster showing the main components. The three characteristic dimensions L , h , and d are also indicated.

end of a coaxial annular dielectric channel that confines the discharge. Xenon is generally used as a propellant gas for its specific properties in terms of high atomic mass and low ionization energy. A set of solenoids provides a radially directed magnetic field \mathbf{B} of which the strength is maximum in the vicinity of the channel exhaust. The magnetic field is chosen strong enough to make the electron Larmor radius much smaller than the discharge chamber length, but weak enough not to affect ion trajectories. The electric potential drop is mostly concentrated in the final section of the channel owing to the low electron axial mobility in this restricted area. The corresponding induced local axial electric field \mathbf{E} has two main effects. First, it drives a high electron azimuthal drift, the Hall current, that is responsible for the efficient ionization of the supplied gas. Second, it accelerates ions out of the channel, which generates thrust. The ion beam is neutralized by a fraction of electrons emitted from the cathode. When operating near 1.5 kW, a HET ejects ions at 20 km s^{-1} and generates 100 mN of thrust with an overall efficiency of about 50%.

HETs are currently employed for geosynchronous satellite attitude correction and station keeping. They also appear as good candidates for the primary propulsion engine of space probes, as demonstrated by the successful SMART-1 moon flyby solar-powered mission [5]. Space agencies together with satellite manufacturers and users nonetheless envisage new fields of application for electric propulsion systems that require low and high-power devices. Low-power Hall thrusters ($\sim 100 \text{ W}$) are well suited for drag compensation of observation satellites that operate on a low-altitude orbit in the Earth atmosphere as well as for trajectory correction of small platforms and microsatellite constellations. The use of high-power ($\sim 5 \text{ kW}$) Hall thrusters for orbit raising and orbit topping maneuvers of communication satellites would offer significant benefits in terms of launch mass, payload mass and operational life. In addition, journeys toward far-off planets and asteroids with large and heavy robotic probes and moon and Mars cargo missions necessitate to build thrusters with an input power in the range of 10–100 kW. In view of the projects demand, it appears necessary to expand the operating envelope of the existing technology to achieve the required performance level. A nontrivial question then arises: How to extrapolate the design and architecture of currently existing Hall thrusters toward different scales and different operating conditions? In other words, what are the scaling relations that connect Hall thruster characteristic dimensions with operating parameters and performances?

II. Overview of Previous Studies and Aim of the Work

Scaling relations that govern the physical properties, the accelerating ability, and the propellant and energy consumption of

Hall thrusters have been extensively investigated by numerous authors since the period of development of Hall thrusters in the '70s. In spite of decades of research on this subject, the assessment of scaling relations is still a topic of interest as various methodologies and results exist. Therefore, before describing the approach associated with this study as well as its outcomes, it is worth briefly reviewing works carried out on this topic during the past few years.

According to the pioneer works of the Russian physicist Morozov and Savelyev [3], to derive scaling relations it is necessary to find a similarity criterion, or a set of criteria, that warrant the underlying physical processes to stay unchanged whatever the thruster. This principle states that the properties of thrusters with a different geometry are linked by way of scaling relations only if a sufficiently large number of dimensionless similarity criteria coincide. The complete set of similarity criteria has not yet been found, however, all works show that the *Melikov–Morozov criterion* has a strong impact on HET behavior and characteristics and it must always be taken into account. This criterion indicates that the ionization mean free path must be less than the channel length ($\lambda_i \ll L$). In addition to similarity criteria, the investigation of scaling laws for Hall thrusters necessitates to account for simplifying assumptions and physical constraints.

Zhurin et al. proposed a sizing method which is limited to the effects of changing either the channel width h or the channel mean diameter d [1]. The channel mean diameter being much larger than the channel width, variation of parameters in the radial direction are negligible. Furthermore, they considered a fixed discharge voltage. To obtain similar performances for two different thruster configurations, authors postulate that the ratio of the Larmor radius r_L , the mean free path λ and the channel length L to channel width h must stay the same for the two configurations. Using these criteria and a set of assumptions they demonstrate that the magnetic field strength is inversely proportional to the channel width $B \propto 1/h$, whereas the discharge current and the propellant mass flow rate are proportional to the channel mean diameter $I_d \propto d$ and $\dot{m} \propto d$.

It was demonstrated by Kim [4] that to reach a high level of efficiency it is not only necessary to ionize and accelerate ions but to accelerate them into the proper direction, hence the need for an optimized magnetic field topology. In short, for a HET with an optimized magnetic field map, there is a relationship between the acceleration layer length L_a and the magnetic layer characteristic size L_B and between L_a and h . The use of these similarity criteria, which include the magnetic field structure, permits to simplify the development of new Hall thruster models. Kim et al. also emphasize the fact that for a traditional HET design the Melikov–Morozov criterion must be fulfilled [6]. Moreover they give additional criteria about the geometry of thruster elements, i.e., the channel length L and mean diameter d are both proportional to the channel width h , that are equivalent to the ones given by Zhurin et al. [1]. There are two immediate consequences. First, the propellant mass flow density and the power density rise when the thruster size decreases, assuming a constant discharge voltage and a constant mass flow rate. Second, as the magnetic field strength is connected with the characteristic dimensions, notably the channel width, and with the operation mode, the magnetic field magnitude must rise when the size reduces to keep comparable conditions.

The method presented by Ashkenazy et al. concerns low-power scaling and it is based on the idea of a sufficient propellant utilization [7]. They show by means of a simplified analysis that a straightforward approach for scaling down the channel size results in a rise of power losses and a reduced overall efficiency. To avoid these effects, the acceleration region has to be scaled down along with the channel width and the magnetic field strength must be increased inversely proportional to the channel width.

Khayms and Martinez-Sanchez developed an approach for low-power thrusters that includes the use of reference points [8]. The goal is to achieve a reduction in the thruster length scale while preserving both the thrust efficiency and the specific impulse. The main result of their study is that the propellant mass flow rate and the applied power scale as the channel length, $\dot{m} \propto L$ and $P \propto L$, whereas the magnetic field strength is in inverse proportion to the latter, $B \propto 1/L$. This

scaling method allows to calculate the channel size and the performances of a small thruster with a given input power provided that a well-known thruster is used as a reference.

Daren et al. suggested an improvement of the existing scaling theory by introducing a scaling index variable [9]. They assume that the electron temperature and the discharge voltage are constant, that the ratio λ_i/L is constant and that the geometric similarity is given by $r/R = \text{constant}$ and $R^{2-\xi}/L = \text{constant}$, where R and r are the channel outer, respectively, inner radius and ξ represents a scaling index variable. They show by way of a comparison of experimental data with numerical outcomes for different values of ξ , that results obtained from their scaling theory agree well with the experimental data for $\xi = 2$. Therefore they deduce that the number density n is constant, whereas the mass flow rate \dot{m} , the input power P , the thrust T and the discharge current I_d are proportional to the square of the outer channel radius R .

Finally, Misuri et al. advised to employ an analytical model coupled to an existing Hall thruster database [10]. This scaling methodology aims to provide design options for high-power thrusters. The idea is to create a vector of fundamental parameters defining the thruster geometry and its performances. This vector is composed of three geometric parameters (L , h , and d), the gas number density in the injection plane and the applied discharge voltage U_d . A scaling matrix derived from the Hall thruster physical principles allows to obtain new thruster characteristics on the basis of a reference thruster.

In a recent article [11], we put forward an original way to extrapolate Hall thruster geometry (L , h , and d quantities) and magnetic field strength toward both the low- and high-power ranges. The approach is based on the combination of a set of scaling relations that are extracted from fundamental equations along with a vast body of existing data. Strong assumptions are made to define the working frame: among others, quantities are steady and homogeneous in the plasma, the applied potential energy is fully converted into axial kinetic energy and all xenon ions are singly charged. Our study indicates both the input power and the thrust scale as hd/L whereas the magnetic field intensity varies as $1/hd$. Besides, realistic constraints on the performance level and on the thermal load are added to limit the set of possible values for the characteristic sizes. In this contribution, the scaling relations and the sizing methodology previously worked out are refined by taking into account an atom density constraint inside the channel and the fact that the channel mean diameter d is proportional to the channel width h . Furthermore, we study the effect of reducing the number of simplifying assumptions. A new set of scaling relations is then given when considering the evolution of the electron temperature T_e , the voltage losses Δ , and the fraction of doubly charged ions f_{2+} as a function of the discharge voltage U_d as well as the ion beam divergence. The two sets of scaling relations obtained under high and low assumptions are subsequently used to determine the geometry and the operating parameters of a 20 kW-class Hall thruster.

III. Set of Governing Relations and Scaling

A. Ionization and Plasma Containment

The geometry of a Hall effect thruster is defined by three characteristic dimensions, namely: the discharge channel length L , the channel mean diameter $d = \frac{1}{2}(d_{\text{ext}} + d_{\text{int}})$, and the channel width h . For the sake of clarity, the three sizes are shown in Fig. 1. As we will see, the thruster geometry depends upon a set of operating parameters such as the discharge voltage U_d and the propellant mass flow rate \dot{m}_n , as well as upon the magnetic field strength B .

A necessary first step to determine scaling relations for Hall thrusters does consist in finding some critical parameters as well as in defining similarity criteria based on the current knowledge and understanding of the physics of Hall thrusters. Therefore, processes at the origin of thrust, must be considered and critically examined. In the remainder of this paragraph, all quantities are assumed to be steady in time and uniform in space to permit the derivation of necessary equations.

1. Propellant Ionization

The first relationship reflecting the impact of the thruster scale on its performance is the relationship between the discharge channel length L and the ionization mean free path λ_i . To ensure a sufficient ionization of the gas, atoms must stay long enough inside the channel. Differently said, it is necessary to satisfy the Melikov–Morozov criterion:

$$\lambda_i \ll L \quad (1)$$

The ionization frequency that originates from electron–atom impacts reads:

$$v_i = n_n \langle \sigma_i(v_e) v_e \rangle \approx n_n \sigma_i(T_e) \sqrt{\frac{8k_B T_e}{\pi m_e}} \quad (2)$$

The ionization length, which corresponds to the mean distance an atom can travel before being ionized, can be formulated as the ratio v_n/v_i in a first-order approximation. Therefore, the Melikov–Morozov criterion can be expressed as:

$$\lambda_i = \frac{v_n(T_n)}{n_n \sigma_i(T_e) v_e(T_e)} \ll L \quad (3)$$

2. Electron Confinement

The magnetic field strength in a Hall effect thruster is such that electrons are magnetized and ions are not, or at least weakly, magnetized. Because ions are much heavier than electrons, the following criterion must be fulfilled [4]:

$$r_{Le} \ll L \quad (4)$$

The definition of the electron Larmor radius is:

$$r_{Le} = \frac{m_e v_e(T_e)}{eB} \quad (5)$$

Keeping the ratio of r_{Le} to L constant, the following relationship can be established:

$$B \propto \frac{m_e v_e(T_e)}{eL} \quad (6)$$

The relation (6) between the magnetic field strength B and the channel length L has already been mentioned by Khayms and Martinez-Sanchez [8].

A second constraint can be established due to the fact that the electron gyroperiod τ_{ce} in the magnetic barrier must be much shorter than the time between two consecutive electron-atom collisions τ_{en} to minimize electron diffusion losses:

$$\frac{\tau_{en}}{\tau_{ce}} = \frac{\omega_{ce}}{v_{en}} = \frac{eB}{m_e n_n \sigma_{en} v_e} \gg 1 \quad (7)$$

where $\omega_{ce} = eB/m_e$ and $v_{en} = n_n \sigma_{en} v_e$ [12]. This point warrants electrons are efficiently trapped inside the magnetic field of a Hall thruster, which is necessary to produce a high electric field and to favor ionization of the seeded gas. In fact, τ_{en} is so long in a HET that anomalous electron transport perpendicular to the magnetic field lines must be put forwards to correctly explain the observed properties and the magnitude of measured quantities [1,3,13]. Equation (7) implies:

$$B \propto \frac{m_e}{e} \sigma_{en}(T_n, T_e) v_e(T_e) n_n \quad (8)$$

This equation indicates that B depends upon the gas density n_n in compliance with the fact that plasma confinement depends on collision events with neutrals. For a given thruster, the higher the gas density inside the channel, i.e., the larger the propellant flow, the stronger the magnetic field must be. Aforementioned equation also shows it is necessary to increase B when the applied voltage is

ramped up as the electron temperature augments with the voltage, see Sec. VII.

3. Neutral Particle Density

The Melikov–Morozov criterion, see Eq. (3), can be used to link the propellant atom number density n_n to the channel length L when keeping the ratio λ_i/L constant for all thrusters. However, two other hypothesis are necessary. The propellant speed v_n and the electron temperature T_e do not depend upon the thruster operating conditions. Whereas the first assumption is reasonable, see, e.g., [14], the second one is only valid at a fixed discharge voltage as discussed in Sec. VII. Thus, Eq. (3) leads to:

$$L \propto \frac{1}{n_n} \quad (9)$$

The relation (9) is similar to the one developed before by, e.g., Zhurin et al. [1] and Khayms and Martinez-Sanchez [8]. It tells the channel length can be decreased when the gas density rises as ionization is favored.

Another relation between n_n and Hall thruster dimensions can be established when considering the propellant mass flow rate passing through the anode \dot{m}_n . The mass flow rate can be decomposed into the product of several terms:

$$\dot{m}_n = n_n \cdot m_n \cdot v_n \cdot A \quad (10)$$

The annular channel cross section A is given by:

$$A = \frac{\pi}{4} (d_{\text{ext}}^2 - d_{\text{int}}^2) = \frac{\pi}{4} \underbrace{(d_{\text{ext}} + d_{\text{int}})}_{2d} \underbrace{(d_{\text{ext}} - d_{\text{int}})}_{2h} = \pi h d \quad (11)$$

We can therefore consider that for a constant atom temperature:

$$n_n \propto \frac{\dot{m}_n}{h d} \quad (12)$$

This relationship between the atom number density and the thruster dimensions h and d has never been mentioned previously, as authors never considered two sizes at the same time. To keep the physical processes at work in a Hall effect thruster unchanged, to warrant a high efficiency and to limit the thermal load as well as the channel wall wear, the number densities of electrons and atoms must stay roughly fixed inside the thruster channel whatever the input power, as we will see in a following paragraph.

B. Relationship Between Performances and Dimensions

The definition of the thrust T , the specific impulse I_{sp} , the various currents, the thrust efficiency η_T , and the anode efficiency η_A can be found in many papers and in most textbooks about electric propulsion (see, e.g., [2,15]). Here we use common definitions to determine the relationships between Hall thruster functioning parameters, performances, and channel characteristic dimensions.

1. Thrust

The thrust is the force supplied by the engine to the spacecraft. It is given by the time rate of change of the momentum since the spacecraft mass varies with time due to propellant consumption. In a Hall thruster, ions originate in the ionization of the propellant gas and they are accelerated by an electric field within the plasma. The thrust therefore results from the electrostatic acceleration of the ions:

$$T = \dot{m}_i \bar{v}_i = \alpha \dot{m}_n \bar{v}_i \quad (13)$$

where the coefficient α stands for the fraction of propellant atoms that are converted into ions, whatever the electric charge. For conventional Hall effect thruster, the typical value of α is around 0.9 with xenon when only singly charged ions are accounted for. Nonetheless, the value of α depends on the discharge voltage [11]. Moreover, it is known that smaller thrusters have a lower propellant conversion efficiency. Notwithstanding the fact that ions are not

magnetized in a Hall thruster, the presence of a transverse magnetic field is responsible for a large azimuthal drift current, also called Hall current. Indeed, electrons in the plasma feel an $\mathbf{E} \times \mathbf{B}$ drift, hence they move perpendicular to the electric and magnetic field [1,2]. The Lorentz force electrons experience is equal to the electrostatic force on the ions, hence:

$$T = \iiint_V \mathbf{j}_{\text{Hall}} \times \mathbf{B} dV \quad (14)$$

$$= 2\pi r \iint_S \mathbf{j}_{\text{Hall}} \times \mathbf{B} dS \quad (15)$$

$$= \pi d I_{\text{Hall}} B \quad (16)$$

To sum up, in a Hall thruster, the thrust is transferred from the ion flow to the thruster body through the magnetic field.

When analyzing the thrust generation in a Hall thruster, one must take into account the presence of multiply charged ion species, especially doubly charged ions [16] of which the fraction is significant with xenon. If the beam contains the two types of ions, the ion mass flow rate is then:

$$\dot{m}_i = \frac{m_n}{e} I^{+} + \frac{m_n}{2e} I^{2+} \quad (17)$$

where the superscript indicates the electrical charge. The thrust can in fact be split into a finite series of elementary terms, each of them corresponding to a given ion species:

$$T = m_n \sum_{k=1}^Z \frac{I^{k+} \bar{v}^{k+}}{k e} \quad (18)$$

where Z is the atomic number. Using the preceding definition for \dot{m}_i , the thrust corrected for the multiple species and for the ion beam divergence can then be written down in the simple form:

$$T = \gamma \theta_d \dot{m}_i \sqrt{\frac{2e}{m_n}} \sqrt{U_d - \Delta} = \alpha \gamma \theta_d \dot{m}_n \sqrt{\frac{2e}{m_n}} \sqrt{U_d - \Delta} \quad (19)$$

where γ is the multiply charged ion correction factor and θ_d is the beam divergence correction factor. The two factors are described in detail in [2]. They naturally depend on the thruster operating conditions. Here, the quantity $(U_d - \Delta)$ is the potential ions really experience. The preceding equation is obtained under the assumption that all types of ions are produced at the same location and therefore undergo the same potential drop. In other words, the voltage losses for ions are independent of the charge number. In that case, the mean ion exhaust velocity can be defined as [3]:

$$\bar{v}_i = \sqrt{\frac{2e}{m_i} (U_d - \Delta)} \quad (20)$$

If one considers solely singly and doubly charged ions, the multiply charged ion correction factor γ reads:

$$\gamma = \frac{1 + \frac{f_{2+}}{\sqrt{2}I^{+}}}{1 + \frac{f_{2+}}{2I^{+}}}, \quad \gamma = \frac{1 + \frac{f_{2+}}{\sqrt{2}(1-f_{2+})}}{1 + \frac{f_{2+}}{2(1-f_{2+})}} \quad (21)$$

Combining Eqs. (10), (11), and (19), yields an expression for the thrust as a function of the channel sizes:

$$T \propto \alpha \gamma \theta_d n_n v_n (T_n) \sqrt{U_d - \Delta} h d \quad (22)$$

As we have shown previously with Eq. (9), varying the atom density n_n corresponds to varying the channel length the opposite way. Therefore, a general relationship between the thrust and Hall thruster characteristic sizes reads:

$$T \propto \alpha \gamma \theta_d v_n(T_n) \frac{1}{L} \sqrt{U_d - \Delta} h d \quad (23)$$

$$\frac{T}{P} \propto \frac{1}{\sqrt{U_d}} \propto \frac{1}{I_{sp}} \quad (33)$$

2. Specific Impulse

The specific impulse is a way to describe the efficiency of rocket and spacecraft engines. It represents the change in momentum per unit of propellant. Essentially, the higher the specific impulse, the less propellant is required to gain a given amount of momentum. In this regard a propulsion method is more propellant-efficient if the specific impulse is higher. The specific impulse is defined by the following equation:

$$I_{sp} = \frac{T}{\dot{m} g_0} \approx \alpha \gamma \theta_d \frac{\bar{v}_i}{g_0} \quad (24)$$

where g_0 is the standard gravity at Earth's surface. Here, \dot{m} refers to the total gas mass flow rate, that means the anode as well as the cathode gas flow rate. When solely the anode mass flow rate is used, strictly speaking the I_{sp} then corresponds to the anode I_{sp} . According to Eq. (19), in a first-order approximation, the specific impulse is not a function of the thruster sizes [11]:

$$I_{sp} \propto \sqrt{U_d - \Delta} \quad (25)$$

It is solely proportional to the square root of the discharge voltage. Note that for a parallel beam of singly charged ion species under the condition of full ionization of the supplied propellant, the specific impulse is simply given by the ratio \bar{v}_i/g_0 . This expression is often found in books and articles.

3. Electrical Power

The discharge current is the sum of the ion current in the beam and the electron current flowing across the channel outlet: $I_d = I_i + I_e$. Neglecting the electronic part, which is a small fraction of the ionic part (typically 10–20%), one can write:

$$I_d \approx I_i = \sum_{k=1}^Z I^{k+} \quad (26)$$

The discharge current can therefore be expressed in terms of propellant mass flow rate:

$$I_d \approx \frac{e}{m_n} \gamma \dot{m}_i = \frac{e}{m_n} \gamma \alpha \dot{m}_n \quad (27)$$

If again solely singly and doubly charged ions are taken into account, the correction factor γ' is given by:

$$\gamma' = \frac{1 + \frac{f_2^+}{f_1^+}}{1 + \frac{f_2^+}{2f_1^+}}, \quad \gamma' = \frac{1 + \frac{f_2^+}{1-f_2^+}}{1 + \frac{f_2^+}{2(1-f_2^+)}} \quad (28)$$

Substituting Eq. (10) into previous equation gives:

$$I_d \approx \pi e \gamma' \alpha n_n v_n(T_n) h d \quad (29)$$

Finally, from the relation between the gas density and the channel sizes, one finds:

$$I_d \propto \gamma' \alpha v_n(T_n) \frac{h d}{L} \quad (30)$$

As a direct consequence, the input electrical discharge power is:

$$P = U_d I_d \quad (31)$$

$$\propto \gamma' \alpha v_n(T_n) \frac{h d}{L} U_d \quad (32)$$

It is worth noticing that for a Hall thruster, the thrust-to-power ratio is not linked to the sizes; it solely depends upon the applied voltage. Voltage losses are always low in comparison with the applied voltage, $\Delta \ll U_d$, hence the thrust per unit input power is:

This last equation shows that for a given input power, increasing the specific impulse reduces the thrust that can be produced.

Preceding relations between the performances and the dimensions are in agreement with those described by Daren et al. [9]. If one considers, as they do, a constant number density n_n , a constant discharge voltage U_d and a geometric similarity such as $R \propto r$, it appears that the thrust, the electrical power and the discharge current vary as the square of the channel mean diameter.

4. Efficiency

The total efficiency, or thrust efficiency, of a Hall thruster is defined as the ratio of the mechanical power to the overall electrical power [2]. It reads:

$$\eta_T = \frac{T^2}{2\dot{m} P_{in}} \quad (34)$$

The mass flow rate \dot{m} accounts for both the anode and the cathode gas flow rate. The total power P_{in} comprises the discharge power P as well as the power dissipated into the coils and for cathode heating. As the last two quantities are much below the discharge power, the thrust efficiency is often given by:

$$\eta_T = \frac{T^2}{2\dot{m} U_d I_d} \quad (35)$$

In this work, only the gas flowing through the injector is considered. The thrust is then expressed as the anode efficiency:

$$\eta_a = \frac{T^2}{2\dot{m}_n U_d I_d} \quad (36)$$

Using the set of available equations for all terms, the anode efficiency appears not to be a function of the Hall thruster channel dimensions:

$$\eta_a \propto \alpha \theta_d^2 \frac{\gamma'^2 U_d - \Delta}{U_d} \neq f(h, d, L) \quad (37)$$

This striking result actually originates from approximations of our model. Especially, the propellant conversion efficiency α and the voltage losses Δ are said not to change with the geometry. It is well known, however, that efficiency has a strong dependence on thruster size: the efficiency is better when the thruster is larger. This fact is directly linked to the volume-to-surface ratio: plasma is produced in volume (so the thrust) and energy is lost on surfaces (i.e., channel walls) by way of particle bombardment and recombination. Neglecting losses at the channel back, the ratio $\frac{V}{S}$ is equal to $\frac{h}{2}$, which explains the gain in efficiency with the size.

IV. Performance and Geometry Data

A. Description of the Database

A thorough open literature search using a wide range of resources combined with data-gathering within the French research program on electric propulsion allowed us to create a large database on Hall effect thrusters. The database contains information about thruster geometry as well as performances, notably the thrust T , the specific impulse I_{sp} and the anode efficiency η_a for a series of 33 different single-stage Hall thrusters. The database also includes information about the magnetic field strength B , the discharge channel wall materials, and the propellant gas. The entire database covers a vast range of input power that stretches from 10 W up to 50 kW and a large collection of data points in terms of applied discharge voltage and gas mass flow rate. A broad range of thrust level is covered, going from 0.4 mN with a micro Hall thruster up to almost 3 N delivered by the high-power thruster developed at NASA. In this work, we focus on Hall thrusters equipped with BN-SiO₂ channel walls and operating with xenon as a propellant gas. A part of the collected data in terms of

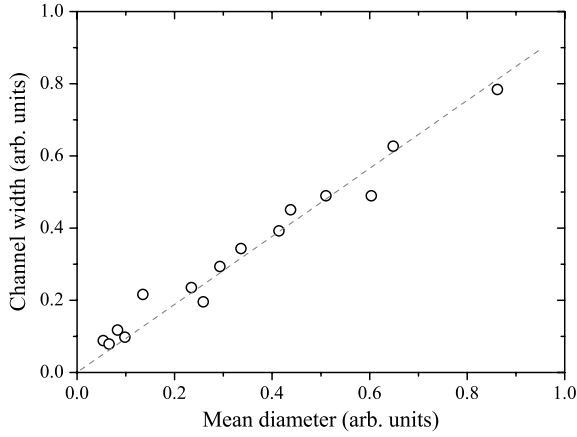


Fig. 2 Channel width h as a function of the channel mean diameter d for a variety of Hall effect thrusters (sizes are in arbitrary units). The two dimensions d and h are proportional.

thrust, specific impulse and thrust efficiency is represented in previous papers [11,15].

B. Dimensional Trends in the Data

It was shown in preceding studies that there is an optimum atomic number density n_n to keep the physical processes at work in a Hall thrusters unchanged, to warrant a high efficiency and to limit the thermal load as well as the wall wear [11,17]. According to the large amount of gathered data, the critical value that turns out to guarantee a satisfying operation is $n_{n,c} = 1.2 \times 10^{19} \text{ m}^{-3}$. This is also the value that is commonly found in literature [2]. When $n_n < n_{n,c}$, the collision events between atoms and electrons are too scarce to maintain a high ionization level. When $n_n > n_{n,c}$, the electron magnetic confinement is weakened due to the high electron-atom collision frequency inside the channel. As the electron diffusion perpendicular to the magnetic field increases, the electric field expands and decreases in strength, the overlap between the ionization and acceleration layers stretches out and the electron back stream through the channel outlet rises. As a consequence, the thruster efficiency drops.

The existence of a critical atom number density $n_{n,c}$ has one direct consequence. According to Eqs. (10) and (11), the channel area is proportional to the gas flow rate: $hd \propto \dot{m}_n$. It confirms that when sizing a Hall thruster, the hd product must follow the evolution of the mass flow rate to ensure a high efficiency. In Fig. 2, the channel width is plotted as a function of the mean diameter for different thrusters covering a broad power range. As can be seen, the two dimensions h and d are in fact proportional. All existing Hall thrusters seem to have a similar d/h ratio whatever the input power. This surprising result could be explained by the fact that the geometry of all Hall thrusters is an extrapolation of a first Russian Hall thruster design. Figure 3 shows the variation of ratio of the mean diameter to the channel width as a function of the normal input power for different thrusters. As can be seen the variation is quite low over a broad range of thruster scales.

Note that, due to $n_{n,c}$, there is also a critical electron number density to ensure an efficient thruster operation. The ionization degree being roughly 10% in a Hall thruster, the critical electron density lies around 10^{18} m^{-3} .

V. Scaling Relations in the Case of High Assumptions

A. List of High Simplifying Assumptions

To simplify the determination of scaling relations, the following assumptions have been made first:

- 1) All quantities are steady in time and uniform in space.
- 2) The electron temperature is unchanging whatever the operating conditions.
- 3) The propellant gas has a uniform and fixed temperature all over the channel, hence a constant propellant velocity.

4) The potential energy is fully converted into kinetic energy and all ions experience the whole potential drop, of which the magnitude is U_d ($\Delta = 0$).

5) Plasma-wall interactions are taken into account through heat load to the channel walls.

6) The magnetic field is uniform; solely its value at the exit plane is considered. The channel length L is therefore the length of the region with magnetic field.

7) Electron transport across the magnetic barrier is considered as classical: no anomalous transport is accounted for within the region of strong magnetic field.

8) There are no multiply charged ions in the plasma ($\gamma = \gamma' = 1$).

9) A parallel monokinetic ion beam is produced, i.e., the plasma jet divergence is null ($\theta_d = 1$).

B. Set of Scaling Relations

The scaling relations are then obtained from equations derived in Sec. III using the set of high assumptions. Therefore they read:

$$T = C_{T1} \dot{m}_n \sqrt{U_d} \quad (38)$$

$$T = C_{T2} \sqrt{U_d} d^2 \quad (39)$$

$$I_{sp} = C_{Isp} \sqrt{U_d} \quad (40)$$

$$I_d = C_I d^2 \quad (41)$$

$$P = C_P U_d d^2 \quad (42)$$

$$L = C_L \lambda_i \quad (43)$$

where C factors are proportionality coefficients. One should keep in mind that all equations are only valid when n_n is considered to be constant and equal to the critical density $n_{n,c}$. The validity of this set of relations can naturally be verified using the database. As an illustration, Fig. 4 displays the thrust as a function of the product $\sqrt{U_d} d^2$ for different thrusters. The dashed line represents a linear fit through all data points. For each thruster some values of T are chosen close to the point of normal operation.

C. Magnetic Field

The magnetic field is treated separately in this work. The scaling relations for the magnetic field strength can be obtained using Eqs. (6), (8), and (12):

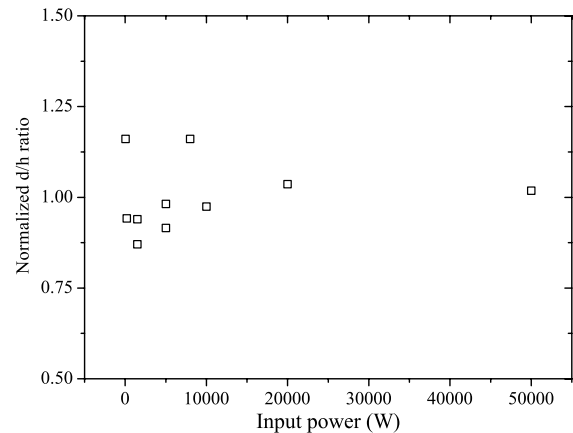


Fig. 3 Normalized ratio of the channel mean diameter to the channel width as a function of the thruster input power.

$$B \propto \dot{m}_n/hd \quad \text{and} \quad B \propto 1/L \quad (44)$$

More general relations are obtained from the set of low assumptions, see Sec. VII:

$$B \propto \dot{m}_n \frac{\sqrt{U_d}}{hd} \quad \text{and} \quad B \propto \frac{\sqrt{U_d}}{L} \quad (45)$$

These relations indicate the field intensity has to be increased for a given thruster geometry when the discharge voltage rises and the propellant flow rate augments to keep a proper plasma confinement. Equations (44) and (45) also show that the magnetic field must be reduced when the thruster sizes increase while keeping the operating conditions of the thruster constant. Nonetheless, according to our database, Hall thrusters operate with a magnetic field strength around typically 200 G, whatever the input power. It is a consequence of the fact that most Hall thrusters operate nominally with a gas density inside the channel close to the critical atom number density $n_{n,c}$. When the atom density is fixed the magnetic field does not depend anymore on the channel diameter d and width h [see Eq. (8)]. It becomes merely a function of the channel length L . Naturally, not only the maximum of the magnetic field determines the thruster efficiency. The entire topology is of relevance. To account for gradients, curvature and position is out of the scope of this study. In the remainder of the paper, B is fixed to 200 G.

D. Assessment of Proportionality Coefficients

To assess the required thruster dimensions by way of a scaling method for an available input power or thrust level, it is thus necessary to know the proportionality coefficients C of the aforementioned equations. These coefficients can be determined either empirically, using the database, or analytically as explained in detail in a previous paper [11]. However, the empirical approach appears to be more accurate.

The empirically determined proportionality coefficients used for sizing a Hall effect thruster are not given in this contribution as it is sensitive information. Only the C_p and C_T coefficients can be derived from outcomes of this study. Yet, they are available in an article previously published by Jankovsky et al. [18].

VI. Sizing of High-Power Hall Thrusters

A. Sizing Methodology

The scaling process that consists in determining the thruster dimensions L , h , and d must be carried out step by step. A detailed description of the procedure is given in another paper [17]. For a fixed discharge voltage and a given thrust level, the standard procedure is the following:

- 1) The required mass flow rate is determined by means of Eq. (38).
- 2) The diameter d is obtained using Eq. (39).
- 3) The discharge current is given by Eq. (41).
- 4) The electric power reads: $P = I_d U_d$.
- 5) The size of h is found using the relationship $h \propto d$.
- 6) The channel length L is assessed with Eq. (43).
- 7) At least, it should be verified that the number density n_n is close to $1.2 \times 10^{19} \text{ m}^{-3}$.

The channel length is the dimension that is the most difficult to determine as the proportionality coefficient C_L can vary over a broad range of values. As has been shown previously [11], the ratio between λ_i and L is not constant but it can vary for different thruster geometry, gas mass flow rate, and discharge voltages. The Melikov–Morozov criterion can, however, be used to get a first estimate of the channel length by using a mean value for C_L determined from the database.

The procedure for a given input power is slightly different. The channel mean diameter can be determined from the given input power. Knowing the mean diameter d one can then determine the thrust level. The remaining thruster dimensions and operating parameters can then be calculated using the equations presented in Sec. V.

B. Thermal Load

During thruster operation a certain percentage of the input power P is lost due to the plasma-wall interactions. Indeed, as shown in [19], a relatively large energy flux q_p is deposited onto the discharge channel walls, mostly due to ion and electron bombardment, which results in a temperature increase of all thruster components. Naturally, there is a maximum amount of power that can be passed to the walls to limit the thermal load and to minimize the sputtering yield of the wall material. One can set a maximum wall temperature T_{\max} above which an efficient operation of a Hall thruster is not possible. The temperature T_{\max} therefore represents a thermal constraint and it must be accounted for when designing a thruster.

A semi-empirical time-dependent thermal model of a Hall effect thruster has been developed to determine the energy flux q_p from a measurement of the temporal evolution of the channel wall temperature [19]. Yet, this model can be used the other way, i.e., to determine the wall temperature from the applied power and the channel size. Here a simplified model of the thruster discharge chamber is used. The thermal enclosure is solely composed of the external and the internal cylindrical walls, meaning that the anode and the rear part of the channel are not taken into account. A more detailed description of the thermal model geometry is given in a previous paper [11].

To assess the channel wall temperature, only the steady-state wall temperature, i.e., the equilibrium temperature, is of relevance, meaning that the transient regime is ignored. The temperature gradient through the walls being weak, thermal exchanges can be modeled considering radiation as the dominant heat transfer mechanism [19]. Knowing the thruster dimensions L , h , and d , the wall temperatures T_{int} and T_{ext} can be computed as a function of the power transferred to the channel walls by the plasma-wall interactions P_{wall} . As it was shown in a previous work [19], the ratio $\frac{P_{\text{wall}}}{P_{\text{input}}}$ is a function of the thruster size and it decreases when the size rises. The process of calculating the wall temperatures can be iterative: in case that the wall temperature is above T_{\max} , the dimensions must be changed until the thermal constraint is satisfied. In this work the maximum temperature for the BN-SiO₂ walls is set to: $T_{\max} = 900 \text{ K}$ in compliance with outcomes of a study on the thermal behavior of a Hall thruster performed a few years ago [20].

C. Design of a 20 kW Hall Thruster

High-power Hall effect thrusters in the range of 10–30 kW and able to deliver a thrust level around 1 N with a specific impulse of about 2500 s, are thought to be used as primary propulsion system for robotic space probes during interplanetary journeys [21,22]. Such high-power Hall thrusters may also be of interest for orbit transfer maneuvers of large satellites. Only a few high-power prototypes have been developed in the world so far and a significant research effort on this specific technology is now appearing within Europe. For this reason, the sizing method based on the aforementioned widely applicable scaling relations in combination with our large database is employed to design a 20 kW-class thruster with a thrust level of 1 N.

The discharge voltage is fixed to $U_d = 500 \text{ V}$ to limit the thermal load and the secondary electron emission. Xenon is used as propellant gas. The thruster channel walls are assumed to be made of BN-SiO₂ ceramics. The wall losses for the thermal constraint are fixed to 4% of the applied power.

The dimensions, the parameters and the estimated performances of a 20 kW-class Hall thruster are given in Table 1. The external wall

Table 1 Computed dimensions, parameters and performances evaluated from scaling relations for a 20 kW thruster delivering 1 N of thrust in the case of high hypothesis. The magnetic field strength is set to 200 G

Dimensions	Parameter	Parameters	Performances
$d = 270 \text{ mm}$	$U_d = 500 \text{ V}$	$P = 17.2 \text{ kW}$	$T = 1 \text{ N}$
$L = 70 \text{ mm}$	$\dot{m} = 41.5 \text{ mg/s}$	$n_n = 1.3 \times 10^{19} \text{ m}^{-3}$	$I_{\text{sp}} = 2456 \text{ s}$
	$I_d = 34.3 \text{ A}$	$T_{\text{wall}} = 670 \text{ K}$	$\eta = 70\%$

temperature is $T_{\text{ext}} = 640$ K and the internal wall temperature is $T_{\text{int}} = 700$ K.

VII. Scaling Relations with Low Assumptions

A. List of Low Assumptions

To investigate the influence of the different assumptions on the scaling model it is worth reducing the list of high assumptions given in Sec. V. It has to be checked if the accuracy of the scaling relations can be improved by using less restrictive assumptions. In the remainder of the work the following assumptions are changed compared with the assumptions presented previously:

- 1) The electron temperature is no longer considered to be constant but it is assumed to increase linearly with the discharge voltage.
- 2) The potential energy is not fully converted into kinetic energy, hence the voltage loss is assumed to be constant and equal 50 V.
- 3) Multiply charged ions are taken into account (γ and $\gamma' = 1$), and the fraction of doubly charged ions is assumed to increase linearly with the voltage.
- 4) The ion beam is no longer considered to be parallel, the beam divergence angle is assumed to be constant and equal to 30° .

B. Available Data and Scaling Relations

Former studies showed that the electron temperature is a function of the applied discharge voltage U_d [23]. Although experimental data about the electron temperature is rare in the literature, we tried to deduce a law on the evolution of T_e as a function of U_d . The electron temperature was measured by a floating movable probe [23] in hot and cold regimes in the plasma plume of different Hall thrusters. The different thrusters are: a 2 kW laboratory model with two different configurations, a narrow (Raitises narrow) and a wide (Raitises wide) one [23] and the NASA-173Mv1 with (NASA-173Mv1¹) and without trim coil (NASA-173Mv1²) [24]. The maximum electron temperature, that is measured in the ionization region, for the different voltages and thrusters is shown in Fig. 5. The evolution of the electron temperature can be assumed to be linear for the different thrusters. A linear fit through all data points gives the following law for the evolution of T_e :

$$T_e = 0.12 \times U_d \quad (46)$$

As can be seen, this linear fit is not quite precise but it is anyhow in good agreement with the common rule-of-thumb that the electron temperature is about one-tenth of the discharge voltage [2]. Therefore it will be used for the determination of the scaling relations. Note that here one assumes a single electron temperature whereas due to the peculiar properties of the crossed-field discharge of a HET one should take into account two electron temperature components: T_e along the magnetic field lines and T_e perpendicular to the field lines.

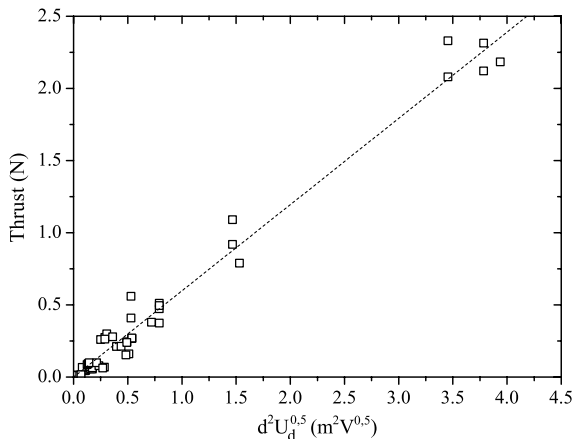


Fig. 4 Thrust as function of $d^2 U_d^{0.5}$ and the linear fit for different Hall effect thrusters (dashed line). For each thruster, some thrust values are chosen around the point of normal operation.

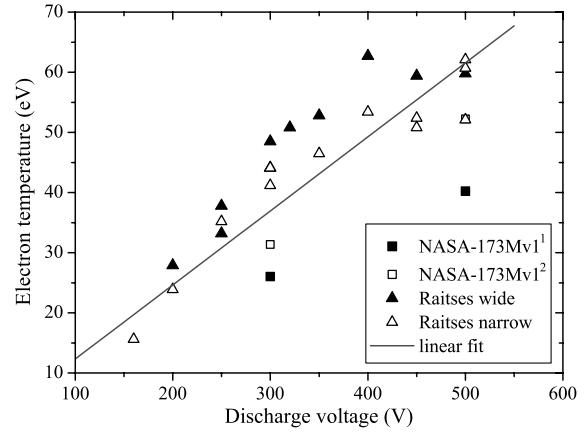


Fig. 5 The maximum electron temperature T_e as a function of the discharge voltage for different Hall thrusters. The equation for the linear fit is: $T_e = 0.12U_d$.

The voltage losses in a Hall effect thruster can be calculated from ion velocity measurements by laser-induced fluorescence or by means of a retarding potential analyzer. Figure 6 shows the evolution of the loss term Δ as a function of the input power. The analyzed thrusters are a SPT100 at a mass flow rate of 2.5 mg/s and the PPS@X000-ML on the one hand for a voltage series at a constant mass flow rate of 6 mg/s and on the other hand for a mass flow series at a constant discharge voltage of 300 V. As can be seen in Fig. 6, voltage losses Δ are more or less fixed for a given thruster geometry and magnetic field map. There is no obvious relation between Δ and thruster size. For the determination of the scaling relations in this work, a constant value of $\Delta = 50$ V is used.

The plasma plume of a Hall thruster contains a nontrivial amount of energetic, multiply charged ions. These multiply charged ions have a higher velocity than singly charged ions when they are accelerated through the same potential drop, which results in a higher erosion rate. The production of multiply charged ions is a loss mechanism for thrust, efficiency and mass flow utilization. Figure 7 shows the evolution of the fraction of doubly charged ions Xe^{2+} as a function of the discharge voltage. The ion species fractions were measured in the NASA-173Mv2 plume far-field by means of an $E \times B$ probe [25]. The measurements were taken with the thruster operating at an anode mass flow rate of 10.0 mg/s. As can be seen in Fig. 7, the Xe^{2+} species fraction f_{2+} increased from 0.04 to 0.12. The evolution of the Xe^{2+} fraction as a function of the discharge voltage can be approximated by the following linear relation:

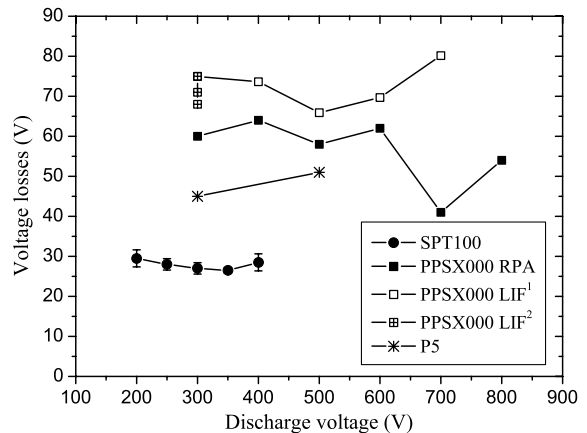


Fig. 6 Voltage losses for the SPT100 and the PPS@ X000-ML measured by RPA and LIF as a function of the discharge voltage. PPS@X000-ML LIF¹ operates at a constant mass flow rate ($\dot{m} = 6$ mg/s), whereas PPS@X000-ML LIF² operates at a constant discharge voltage ($U_d = 300$ V).

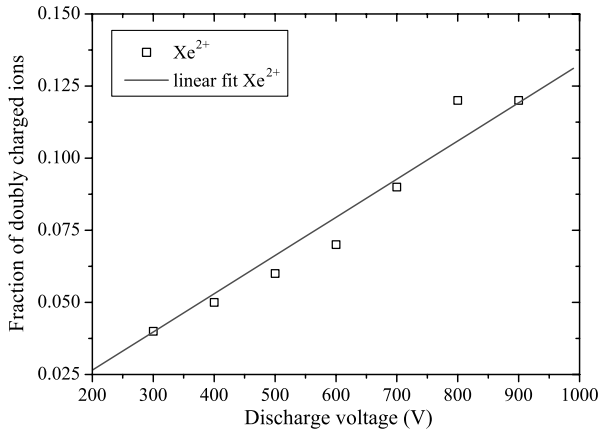


Fig. 7 Fraction of doubly charged ions as a function of the discharge voltage for the NASA-173Mv2 at a mass flow rate of 10 mg/s.

$$f_{Xe^{2+}} = 1.325 \times 10^{-4} U_d \quad (47)$$

The beam divergence angle is set to 30° . Considering an ion beam that diverges uniformly upon the exit of the discharge channel, the beam divergence correction factor is: $\theta_d = \cos(30^\circ) = \frac{\sqrt{3}}{2}$.

The scaling relations in the case of low assumptions can then be obtained from the equations in Sec. III in combination with the list of low assumptions mentioned above and the relations between T_e , Δ , and f_{2+} and the discharge voltage U_d

$$T = C_{T1}^* \gamma \theta_d \dot{m}_n \sqrt{U_d - \Delta} \quad (48)$$

$$T = C_{T2}^* \gamma \theta_d \frac{1}{\sqrt{U_d}} \sqrt{U_d - \Delta} \frac{d^2}{L} \quad (49)$$

$$I_{sp} = C_{Isp}^* \gamma \theta_d \sqrt{U_d - \Delta} \quad (50)$$

$$I_d = C_{I}^* \gamma' \frac{1}{\sqrt{U_d}} \frac{d^2}{L} \quad (51)$$

$$P = C_P^* \gamma' \sqrt{U_d} \frac{d^2}{L} \quad (52)$$

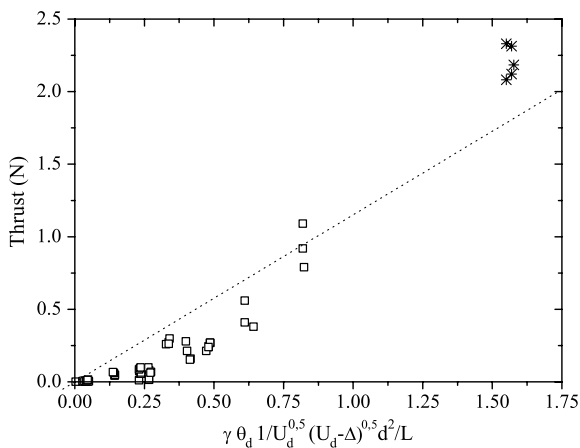


Fig. 8 Thrust as function of $\gamma \theta_d / U_d^{0.5} (U_d - \Delta)^{0.5} d^2 / L$ and the linear fit for different Hall effect thrusters (dashed line). For each thruster, some thrust values are chosen around the point of normal operation. The NASA-457M thruster is represented by the asterisk symbol.

Table 2 Dimensions, parameters, and performances evaluated from scaling relations under low assumptions for a 20 kW thruster delivering 1 N of thrust. The magnetic field strength is fixed to 200 G.

Dimensions	Parameter	Parameters	Performances
$d = 324$ mm	$U_d = 500$ V	$P = 16.8$ kW	$T = 1$ N
$L = 101$ mm	$\dot{m}_d = 49.19$ mg/s	$n_n = 1.2 \times 10^{19}$ m $^{-3}$	$I_{sp} = 2072$ s
	$I_d = 33.65$ A	$T_{wall} = 707.5$ K	$\eta = 61\%$

$$L = \frac{C_L^*}{\sqrt{U_d}} \quad (53)$$

Again the validity of these relations can be verified using the database. Figure 8 shows the thrust as a function of the product $\gamma \theta_d \frac{1}{\sqrt{U_d}} \sqrt{U_d - \Delta} \frac{d^2}{L}$ for different thrusters. The dashed line represents a linear fit through all datapoints. As can be seen in Fig. 8 the datapoints for the NASA-457M thruster are slightly above the datapoints for the other thrusters. The NASA-457M was in fact designed to be used either with xenon or with krypton. Krypton has a lower mass and a higher ionization energy than xenon, thus the discharge channel must be longer. The channel length of the NASA-457M is probably a tradeoff for the two propellants.

C. Sizing of a 20 kW Hall Thruster

The scaling relations developed using the low assumptions are used for the design of a 20 kW-class Hall thrusters to be able to compare the outcomes from the two sizing methods and to estimate the impact of the simplifying assumptions. The design-procedure under low assumptions is slightly different. For a fixed discharge voltage of $U_d = 500$ V and a given thrust level, the product $\frac{d^2}{L}$ can be determined using Eq. (49). The mass flow rate, the specific impulse and the discharge current can be determined using the Eqs. (48), (50), and (51) given above. Assuming an atomic number density of $n_n = 1.2 \times 10^{19}$ m $^{-3}$ the channel mean diameter can then be calculated from the mass flow rate.

The dimensions, the operating parameters and the performances of the 20 kW thruster with a thrust of 1 N are listed in Table 2. The external wall temperature is $T_{ext} = 670$ K and the internal wall temperature is $T_{int} = 745$ K.

D. Comparison Between the Two Approaches

When comparing the results for the two sets of scaling relations (see Tables 1 and 2), one can see there are differences for the operating conditions as well as for the characteristic dimensions of a 20 kW Hall thruster. Solely the value for the discharge current I_d stays almost unchanged. As voltage losses and the divergence angle are taken into account in the case of low assumptions, the required mass flow rate is larger whereas the specific impulse is lower. The characteristic dimensions are bigger in the case of low assumptions. However, the two scaling approaches are in fact in reasonable agreement as these scaling relations are solely supposed to give a first estimation of the required thruster dimensions and operating conditions. As can be seen in Figs. 4 and 8 both set of scaling relations are able to reproduce experimental data over a broad range of power. The accuracy of the scaling relations in the case of low assumptions is, however, lower. One reason for this is the error introduced due to the lack of a sufficiently large number of experimental data; this is especially true for the relation between the electron temperature and the discharge voltage. The last approach also suffers from other sources of inaccuracy. The evolution of voltage losses with sizes is disregarded whereas Δ is less for larger thrusters. Changes in the ion beam divergence with operating conditions and geometry is not considered. In summary, to get a first estimation of the characteristic dimensions and operating conditions for a given input power or a given thrust level, the scaling relations developed in the case of high assumptions are likely sufficient.

VIII. Conclusions

The Hall effect thruster sizing method described in this work considers the three characteristic thruster dimensions L , d and h , as well as the magnetic field strength B . The method relies on analytical laws that are established from the fundamental principles that govern the physics of a Hall thruster in the frame of simplifying assumptions. Besides, the approach must fulfill stringent rules about atomic number density and channel wall temperature. A vast database that encompasses 33 single-stage Hall thrusters covering a power range between 10 W and 50 kW allows to check the validity of the developed scaling relations and to determine the values of the corresponding proportionality coefficients necessary to dimension a new thruster. In this work, two different sets of scaling relations are presented, one in the case of high assumptions and the other in case of low assumptions. Both sets of scaling relations are employed to obtain a first estimate of characteristic dimensions, operating parameters and performances of a 20 kW-class Hall thruster. A comparison of the two methods reveals that reducing the number of assumptions does not lead to an improvement of the accuracy. Scaling relations under high assumptions are therefore satisfactory to get a first estimate of the geometry and the operating conditions of a thruster, which permits to save time during the design and optimization phases.

Acknowledgments

This work is carried out in the frame of the CNRS/CNES/SNECMA/Universités joint research program 3161 Propulsion par Plasma dans l'Espace. It is also part of the High Power Electric Propulsion: A Roadmap for the Future collaborative project financially supported in the frame of the 7th European Framework Program under the grant number 218859.

References

- [1] Zhurin, V. V., Kaufmann, H. R., and Robinson, R. S., "Physics of Closed Drift Thrusters," *Plasma Sources Science and Technology*, Vol. 8, 1999, pp. R1–R2. doi:10.1088/0963-0252/8/1/021
- [2] Goebel, D. M., and Katz, I., *Fundamentals of Electric Propulsion*, Wiley, Hoboken, NJ, 2008.
- [3] Morozov, A. I., and Savelyev, V. V., "Fundamentals of Stationary Plasma Thruster Theory," *Reviews of Plasma Physics*, Vol. 21, edited by B. B. Kadomtsev and V. D. Shafranov, Springer, New York, 2000.
- [4] Kim, V., "Main Physical Features and Processes Determining the Performance of Stationary Plasma Thrusters," *Journal of Propulsion and Power*, Vol. 14, No. 5, 1998, pp. 736–743. doi:10.2514/2.5335
- [5] Koppel, C. R., Marchandise, F., Prioul, M., Estublier, D., and Darnon, F., "The SMART-1 Electric Propulsion Subsystem Around the Moon: In Flight Experience," *Proceedings of the 41th Joint Propulsion Conference*, AIAA Paper 05-3671, 2005.
- [6] Kim, V., Kozlov, V., and Skrylnikov, A., et al., "Development and Investigation of the SPT-20 and SPT-25 Laboratory Models," *Proceedings of the 1st Annual International Conference and Exhibition. Small Satellites: New Technologies, Achievements, Problems and Prospects for the International Cooperation in the New Millennium*, Moscow, 2000.
- [7] Ashkenazy, J., Raitses, Y., and Appelbaum, G., "Low Power Scaling of Hall Thrusters," *Proceedings of the 2nd European Spacecraft Propulsion Conference*, ESA Publications Division, Noordwijk, The Netherlands, 1997.
- [8] Khayms, V., and Martinez-Sanchez, M., "Design of Miniaturized Hall Thruster for Microsatellites," *Proceedings of the 32nd Joint Propulsion Conference*, AIAA Paper 96-3291, 1996.
- [9] Daren, Y., Yongjie, D., and Zhi, Z., "Improvement on the Scaling Theory of the Stationary Plasma Thruster," *Journal of Propulsion and Power*, Vol. 21, No. 1, 2005, pp. 139–143. doi:10.2514/1.5901
- [10] Misuri, T., Battista, F., Barbieri, C., De Marco, E. A., and Andreucci, M., "High Power Hall Thruster Design Options," *Proceedings of the 30th International Electric Propulsion Conference*, IEPC Paper 07-311, 2007.
- [11] Dannenmayer, K., and Mazouffre, S., "Sizing of Hall Effect Thrusters with Input Power and Thrust Level: An Empirical Approach," *Journal of Technical Physics*, Vol. 49, Nos. 3–4, 2008, pp. 231–254.
- [12] Lieberman, M. A., and Lichtenberg, A. J., *Principles of Plasma Discharges and Materials Processing*, Wiley, New York, 1994.
- [13] Koo, J. W., and Boyd, I. D., "Modelling of Anomalous Electron Mobility in Hall Thrusters," *Physics of Plasmas*, Vol. 13, No. 3, 2006.
- [14] Hargus, W. A. Jr., and Cappelli, M. A., "Laser-Induced Fluorescence Measurements of Velocity Within a Hall Discharge," *Applied Physics B*, Vol. 72, No. 8, 2001, pp. 961–969. doi:10.1007/s003400100589.
- [15] Mazouffre, S., Lazurenko, A., Lasgorceix, P., Dudeck, M., d'Esquivan, S., and Duchemin, O., "Expanding Frontiers: Towards High Power Hall Effect Thrusters for Interplanetary Journeys," *Proceedings of the 7th International Symposium on Launcher Technologies*, CNES, Barcelona, Spain, Paper O-25, 2007.
- [16] Gallimore, A., "Near- and Far-Field Characterization of Stationary Plasma Thruster Plumes," *Journal of Spacecraft and Rockets*, Vol. 38, No. 3, 2001, pp. 441–453. doi:10.2514/2.3703
- [17] Dannenmayer, K., and Mazouffre, S., "Elementary Scaling Laws for Sizing Up and Down Hall Effect Thrusters: Impact of Simplifying Assumptions," *Proceedings of the 31st International Electric Propulsion Conference*, IEPC Paper 2009-077, 2009.
- [18] Jankovsky, R. S., Tverdokhlebov, S., and Manzella, D., "High Power Hall Thruster," *Proceedings of the 35th Joint Propulsion Conference*, AIAA Paper 99-2949, 1999.
- [19] Mazouffre, S., Dannenmayer, K., and Pérez-Luna, J., "Examination of Plasma-Wall Interactions in Hall Effect Thrusters by Means of Calibrated Thermal Imaging," *Journal of Applied Physics*, Vol. 102, No. 2, 2007, pp. 023304–1, 023304–10. 23304. doi:10.1063/1.2757716
- [20] Mazouffre, S., Echegut, P., and Dudeck, M., "A Calibrated Infrared Imaging Study on the Steady State Thermal Behavior of Hall Effect Thrusters," *Plasma Sources Science and Technology*, Vol. 16, No. 1, 2007, pp. 13–22. doi:10.1088/0963-0252/16/1/003
- [21] Witzberger, K. E., and Manzella, D., "Performances of Solar Electric Powered Deep Space Missions Using Hall Thruster Propulsion," *Proceedings of the 41st Joint Propulsion Conference*, AIAA Paper 05-4268, Tucson, Arizona, 2005.
- [22] Johnson, L., Meyer, R. A., and Frame, K., "In-Space Propulsion Technologies for Robotic Exploration of the Solar System," *Proceedings of the 42nd Joint Propulsion Conference*, AIAA Paper 06-4687, 2006.
- [23] Raitses, Y., Staack, D., Keidar, M., and Fisch, N. J., "Electron-Wall Interaction in Hall Thrusters," *Physics of Plasmas*, Vol. 12, 2005, pp. 057104–1, 057104–9. doi:10.1063/1.1891747
- [24] Linnel, J. A., and Gallimore, A. D., "Internal Plasma Potential Measurement of a Hall Thruster Using Plasma Lens Focusing," *Physics of Plasmas*, Vol. 13, No. , 2006, pp. 103504–1, 103504–9.
- [25] Hofer, R. R., and Gallimore, A. D., "Ion Species Fractions in the Far-Field Plume of a High-Specific Impulse Hall Thruster," *39th Joint Propulsion Conference*, AIAA Paper 03-5001, 2003.

A. Gallimore
Associate Editor